Investigations of Arcing Phenomena In the Region Near CEBAF RF Windows at 2 K

Tom Powers, Lawrence R. Doolittle, Peter Kneisel,
Viet Nguyen-Tuong, Larry Phillips, and Charles Reece

Continuous Electron Beam Accelerator Facility
12000 Jefferson Ave.
Newport News, VA 23606

Introduction

Several lines of study were undertaken to improve the understanding of arcing phenomena in the region of the CEBAF 2 K rf window. Of special interest was the window performance at levels of cavity power dissipation considerably above normal operating conditions. This paper discusses the results of five of these studies. Some of this data has been previously reported [1, 2, 3, 4]. Two of the studies were carried out using the standard CEBAF cavity-window configuration mounted in a cryomodule. One series was performed using a 5-cell CEBAF cavity with standard ceramic window and a variable rf-coupler tested vertically. The third study used a single-cell cavity with a standard ceramic window and variable rf-coupler, and the final study used a standard cryomodule waveguide and window assembly without a cavity.

A variety of transient electronic activity was observed to occur at or near the rf window, including the emission of light, a precipitous increase in reflected power, and interesting cooperative effects between the window and cavity. Often the initiation of activity at the window is correlated with the presence of a high x-radiation flux that has a duration of less than a few microseconds which is accompanied by a sudden (200 ns to 5 μs) loss of cavity stored energy and a short (tens of microseconds) intense light pulse. An "electronic quench" is the term that we have used when discussing this type of event. The other type of event which was observed has a short intense light pulse followed by a less intense emission which lasts several hundred microseconds. This type of event, which we refer to as a "waveguide vacuum arc" is accompanied by a sudden rise in waveguide vacuum pressure, a more gradual loss of cavity stored energy (300 μs to 600 μs) and occasionally a less intense x-radiation pulse.

Background

The CEBAF ceramic rf-windows are operated at 2 K and close to the beam line. In the presence of field emission in the cavity, a flash of light is occasionally observed in the guard vacuum space which is located between the cold and warm rf windows. This phenomenon is generally referred to as arcing. It was expected that arcing would be a possible issue with the operation of the CEBAF accelerator as it is in many accelerators. The standard arc detection scheme used at CEBAF employs a 931B photomultiplier tube with signal amplitude and duration discrimination. The detection circuits are coupled into the local rf control circuitry, which disables the rf drive to the offending cavity and the fast shut down system which interrupts the beam at the injector. While tests determined that 2.5 μs optical pulse length discrimination would eliminate non-RF induced events, the duration was increased to 50 μs to avoid faults from non-sustained light signals. It should be noted that the potential energy delivered by the 5 kW klystron during this time is a small fraction of the cavity stored energy.

*This work supported by US DOE contract DE-AC05-84ER40150

Cryomodule and Cryounit Test Setups

One set of tests was conducted on cryomodule 17 in December 1992. The cryounit test was conducted in February 1993. The cavity transmitted power signal (P_T), cavity input coupler reflected power signal (P_R), klystron drive signal (P_O) and photomultiplier tube signal were monitored. The PMT anode current was conditioned with a high speed line driver, located in the sensor head, which had a current to voltage transfer function of 1000 V/A. This driver becomes non-linear beyond an output voltage of 0.4 V for the cryomodule test and 10 V for the cryounit test.

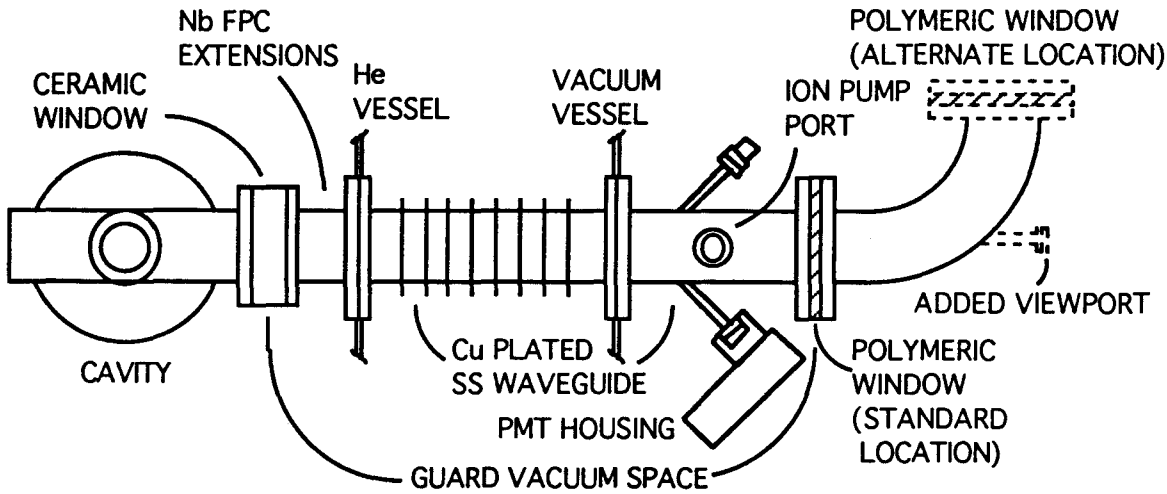

Figure 1. Cavity waveguide configuration for CEBAF cryomodule, showing arc detector, PMT housing alternate location for polymeric window and extra sapphire viewing port (not to scale).

In the cryomodule test and for most of the cryounit data, the optical path from the ceramic window to the sapphire view port is not direct and the port actually views a small area of the copper plated waveguide. See Figure 1. No optical fibers were used, and the PMT housing was mounted directly to the flange of the sapphire window. The rf power sources were two 2 kW klystrons driven by a pair of VCO phase-locked loop subsystems, permitting the independent excitation of two cavities. The design value for the external Q of the fundamental power coupler is 6.6×10^6. This leads to cavity fill and decay times of 700 μs. Figure 2 is an example of the normal turn-off transients associated with a cavity in the cryomodule test. The warm waveguide, at atmospheric pressure, is separated from the guard vacuum by a polymeric window. The guard vacuums on a pair of cavities share a 20 l/s ion pump, which provides a fault signal that interrupts the rf drive when the pressure exceeds 10^{-7} Torr.

The cryounit test was a dedicated test in which two cavities were operated for an extended period of time at electric field levels that exceeded CEBAF design values by 75% and 100%, respectively. The test setup was the same as the cryomodule test with the following exceptions. The standard waveguide elbow on one of the cavities was replaced by an elbow with a cutoff tube and sapphire view port placed so as to have a direct view of the cold window. The polymeric window was moved to the klystron end of the waveguide elbow. A fast rise time scintillator/ photomultiplier tube assembly was placed in various positions around the cavity and the signal was monitored using a digital oscilloscope for transients and pulse counting electronics for steady state measurements. Additionally, the motorized phase shifters in the rf control electronics were replaced with manual phase shifters to reduce induced waveguide vacuum arcs which will be discussed later in this paper.

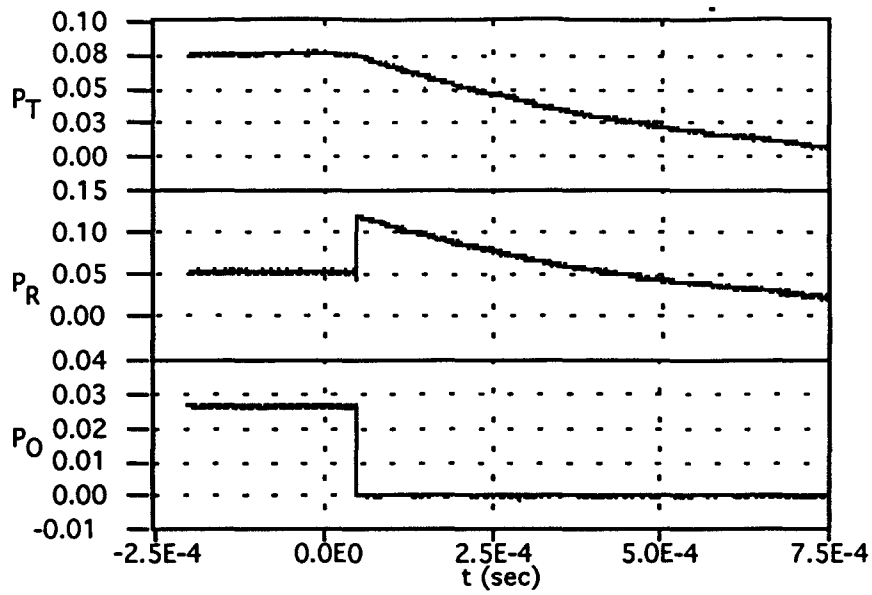

Figure 2. Typical turn-off transients for transmitted power (P_T), reflected power (P_R), and klystron drive (P_O) signals in a cryomodule test. The rf drive (P_O) is turned off at t = 50 μs.

Vertical Test Setups

The dedicated 5-cell vertical test and the cryomodule tests use the same cavity, cold window, and transmitted power field probe configuration. The single-cell vertical test does not have higher order mode (HOM) load couplers, and the field probe is placed on the beam pipe endplate. In both vertical tests (5-cell and single-cell) a cold Nb waveguide-to-coax adapter (tophat) is attached to the ceramic window. Each tophat has a pumping port and a variable coaxial rf coupler which allows for the rf power to be critically coupled to the cavity. Prior to cooldown the valves between the external pumps and the cavity and waveguide vacuum spaces are closed, and any additional pumping is by cryosorption to the walls of the cavity, the tophat and the two pump-out pipes.

Additionally, the tophats have one (single-cell test) or two (5-cell test) Nb cutoff tubes with welded miniconflat flanges to which sapphire windows are attached. These ports allow one to view the ceramic window directly via 2 mm diameter acrylic fibers which transmit light between 375 nm and 700 nm.[2] Additionally, the vertical tests were instrumented with a number of silicon photodiodes, Hamamatsu A1223-01, placed on the cavity, window frame and on the end plates which were used as x-radiation detectors.[5] These sensors were conditioned by two types of amplifiers. The first was a high gain, 20 kHz bandwidth amplifier which had a current to voltage transfer ratio of 15 V/μA. The second, which was used to monitor the field emission radiation levels, was a high gain 100 Hz bandwidth amplifier with a current to voltage transfer ratio of 2.5 V/nA. The rf energy for these tests comes from solid state amplifiers capable of delivering up to 100 W to the cavities.

In the vertical tests the rf power is not interrupted after an arc fault. However, the incident power is limited to approximately 100 W and the external Q of the input coupler is $>10^9$. In the cryomodule tests, as in the accelerator, the rf power is interrupted within a few microseconds of detection of an arc fault. The same optical detectors, 931B photomultiplier tubes, arc discrimination circuits, crystal detectors and data acquisition hardware were used in all setups. The single-cell test and the cryounit test both used PMT preamplifiers which were limited to 10 V while the cryomodule and 5-cell tests were limited to 0.4 V. The steady state electromagnetic field configuration in the cavity, fundamental

power coupler, cold window and the vacuum space around the cold window are the same in all four test setups.

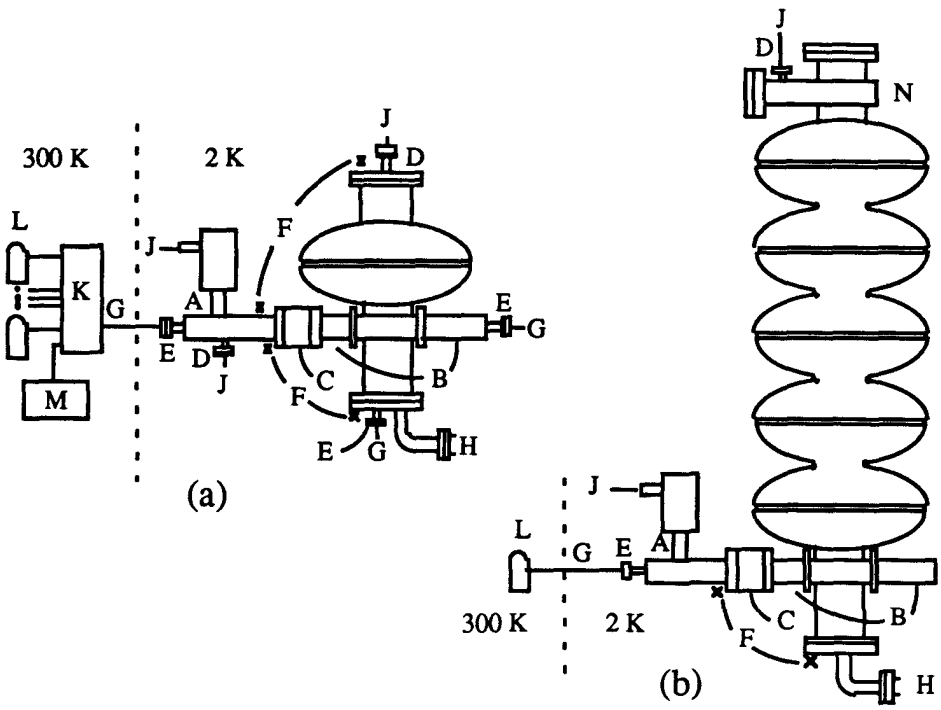

Figure 3. Diagram of (a) single-cell cavity and (b) 5-cell cavity showing (A) top hat with variable coupler, (B) fundamental power coupler, (C) ceramic window, (D) field probe locations, (E) optical windows, (F) x-radiation detectors, (G) fiber optic bundles, (H) cavity pump-out port, (J) rf cables, (K) optical splitter, (L) photomultiplier assembly, (M) monochromator and (N) higher order mode coupler.

Water Vapor Loading Test

Sustained local discharges in rf systems require a source of adsorbed gas. The gas load due to permeation through the polymeric warm windows was measured to be 1.6×10^{-7} Torr-l/sec.[4] Some of this gas is cryopumped onto the inside walls of the waveguide transition and onto the surface of the cold window. Any discharge process inside the waveguide vacuum space probably involves this frozen gas. The water vapor loading test was performed to investigate this phenomenon independent of cavity interactions. The test made use of a waveguide assembly that was configured the same as the cryomodule. The cavity was removed and a shorting plate was added which caused an electric field maximum to be located at the cold window. The same PMTs and detection circuitry were used and up to 2 kW (forward power) was applied to the system. A controlled leak of water vapor was attached in the pumping line, the ceramic window assembly was cooled to about 100 K and water was introduced into the system such that the window was coated with a layer of ice up to 0.5 mm thick. Rf was applied to the system and no arcs were observed during the 80 hours of operation. We concluded from these tests that ice, by itself, was not sufficient to cause arcs.

Oil Drop Test

In this test a single-cell cavity was assembled and tested vertically. The cavity performed well with no arcs or field emission to field levels of 22.5 MV/m (peak surface

field). The cavity was warmed to room temperature and a mist of a solution of one drop of high vacuum oil and one pint of acetone was sprayed on the waveguide side of the window. In the subsequent test the cavity performance degraded as shown in Figure 4. When operated at high fields the cavity arced every two minutes. Additionally, at the completion of the test the window had several through leaks. Figure 4 is a plot of Q vs. E for the two tests.

The problem of contamination by oils on high power rf structures has been investigated previously.[6, 7] While these studies focused on the issues of electron multipactor discharges, they also discussed examples of gas discharges which are initiated by an electron multipactor. In the study by Woode *et al.* [7] the effects of different contaminants and coatings on the inception of a discharge were investigated. It was reported that the most destructive contaminate tested, which caused a 4.3 dB reduction in the onset of a discharge, was the lubricant (oleamide) contained within plastic bags. This reduction occurred after the surface was in direct contact with the plastic bag for 6 hours. Even storing the material in the bag for 12 days, with no direct contact, reduced the threshold by 2.4 dB with no conditioning or subsequent recovery.

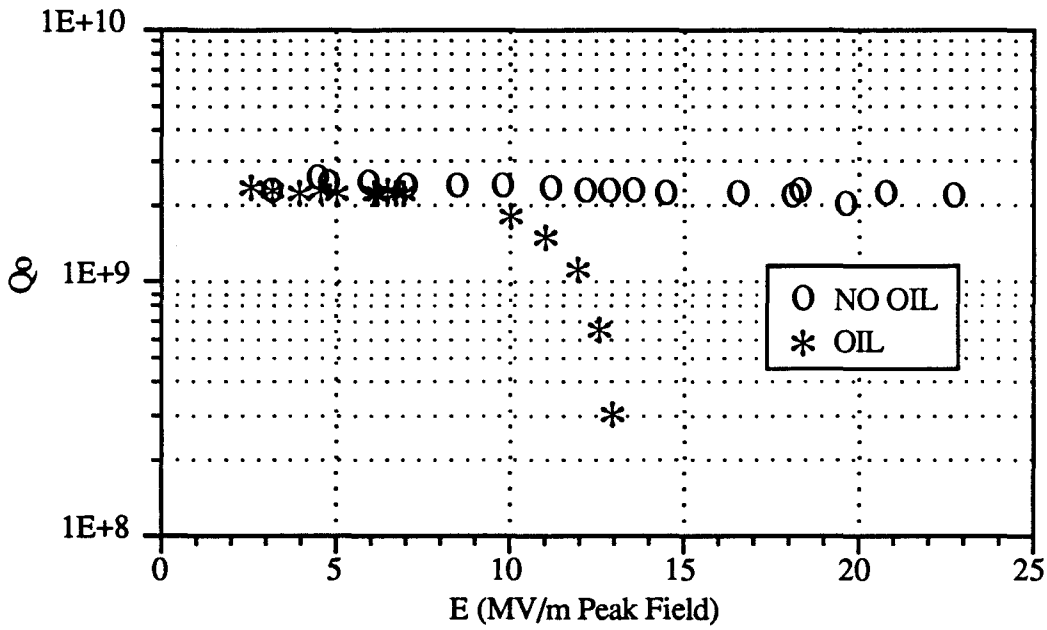

Figure 4 Plot of Q vs. E (peak surface field) for a single-cell cavity before and after the application of an oil and acetone solution to the external face of the window.

Operational Characteristics

In a superconducting cavity, a thermal quench occurs when a localized region of the cavity transitions from the superconducting to the normal conducting state, quickly dissipating the stored energy. This process normally takes at least several hundred microseconds. During the vertical tests, a new type of quench process was identified. In this quench, the stored energy, as measured by the transmitted power signal, is fully dissipated in a time ranging from 150 ns to 5 μs. This is accompanied by a large x-radiation pulse (possibly as large as 500 kRad/hr). We label this phenomenon an electronic quench. Such quenches were strongly correlated with arcing during the dedicated tests. However, they were also observed during rf processing of production cavities where an electronic quench was often associated with a discrete "jump" in cavity performance (E and Q improve with constant input power and coupling).

The vertical arcing tests were run on two cavities over several months with approximately 100 hours of cavity operation. Several hundred events were recorded both with and without light emission. In these tests the cavities were typically operated at or near the maximum field level determined by heavy field emission loading. Under such extreme conditions arcs occurred as frequently as every ten minutes. On some cavities the event rate "conditioned" as the cavity is operated at these high field levels. Figure 5 shows the conditioning that occurred when a cavity was operated at 80% of the maximum attainable electric field level. Conditioning did not always occur when cavities were operated at high levels of field emission. However, systematic studies of conditioning during the initial application of high levels of rf power were not performed.

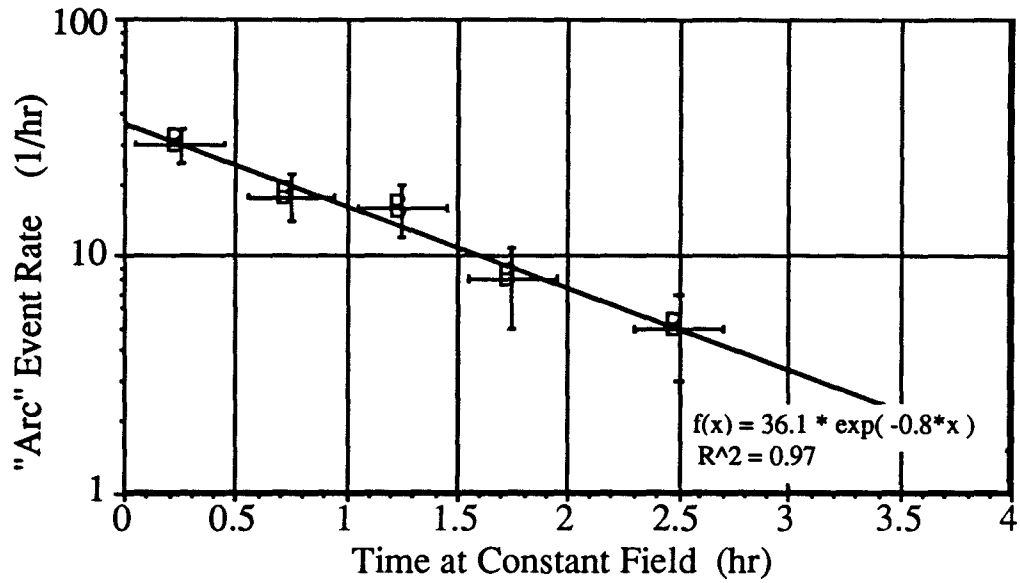

Figure 5. Processing of window arcing in a CEBAF 5-cell cavity tested vertically at a field level of 9.3 MV/m with a constant field emission radiation level.

The cryomodule arcing tests were run parasitically with the normal production testing of the cryomodule cavity performance, heat loads, instrumentation, and tuners. An extended run of three hours with two cavities operated at 5 MV/m was conducted so that a sustained heat load measurement could be taken. The cavities were only run at extreme (at or near maximum) field levels for short periods of time. "Arcing" and "quenches" occurred as the field levels approached their maximum values. No arcs were recorded during the extended run until the field levels were increased and the cavity began to field emit. Approximately 50 light emitting events were recorded.

In the cryounit tests the cavities were initially operated for eight hours at various field levels (two hours at each level) in order to determine the levels possible for the extended high power runs. It was determined that the maximum field level for cavity A was 8.6 MV/m while cavity B reached 10.5 MV/m. Both were limited only by the available rf power. Figure 6 shows the plots of Q vs. E for the two cavities. The low Q values were attributed to residual ambient magnetic fields. The cavities were run at 5 MV/m for 3 hours, 7.5 MV/m for 42 hours, and at maximum field levels of 8.6 MV/m and 10.6 M/m for 4 hours. The cavities were also operated at field levels between 6 MV/m and maximum field levels for an additional 17 hours. Data was recorded whenever there was an arc.

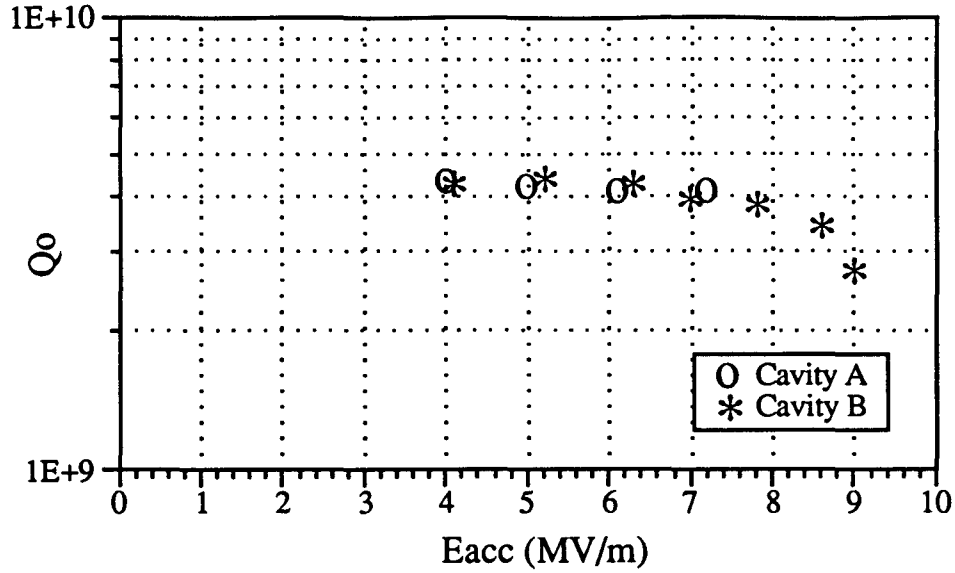

Figure 6. Q_0 vs. E plot for the cavities used in the cryounit tests as measured calorimetricly at the end of the test.

Experimental Results

Summary

Generally, five types of events generally referred to as "arcs" have been identified.

(1) A short (5 - 25 μs), broadband, light pulse with a long (3- 5 ms) narrowband decaying tail which is accompanied by a short (<25 μs) large (possibly 500 kRad/hr) magnitude x-radiation pulse and a rapid (<200 ns) loss of cavity stored energy.

(2) A sustained (4 - 250 μs), broadband, light pulse with a long (3- 5 ms) narrow band decaying tail which is accompanied by a short (<25 μs) moderately large x-radiation pulse (detector currents an order of magnitude less than type 1 events) and a loss of cavity stored energy which had a time constant that matches that of the sustained broadband light pulse.

(3) A rapid (<200 ns) loss of cavity stored energy with no light emission and a short (<25 μs) large (100 - 500 kRad/hr) magnitude x-radiation pulse.

(4) A long (3 - 5 ms) light pulse with no measurable change in the cavity stored energy (<1%), reflected power signal, and x-radiation pulse.

(5) A short (<20 μs) light pulse with no measurable change in the cavity stored energy, reflected power signal, and x-radiation.

The types of events observed during vertical testing were also seen during the cryomodule tests. The three types of events which were exceptions were electronic quenches not accompanied by light that were seen only in the vertical tests, control system induced arcs that were seen in the cryomodule and cryounit tests, and electronic quenches followed by a waveguide vacuum arc which were seen in the cryomodule and cryounit tests. In all tests, arcs and electronic quenches, independent of control system transients, were only observed while a cavity was field emitting accompanied by abundant x-radiation, typically 100 - 500 Rad/hr at the window frame.

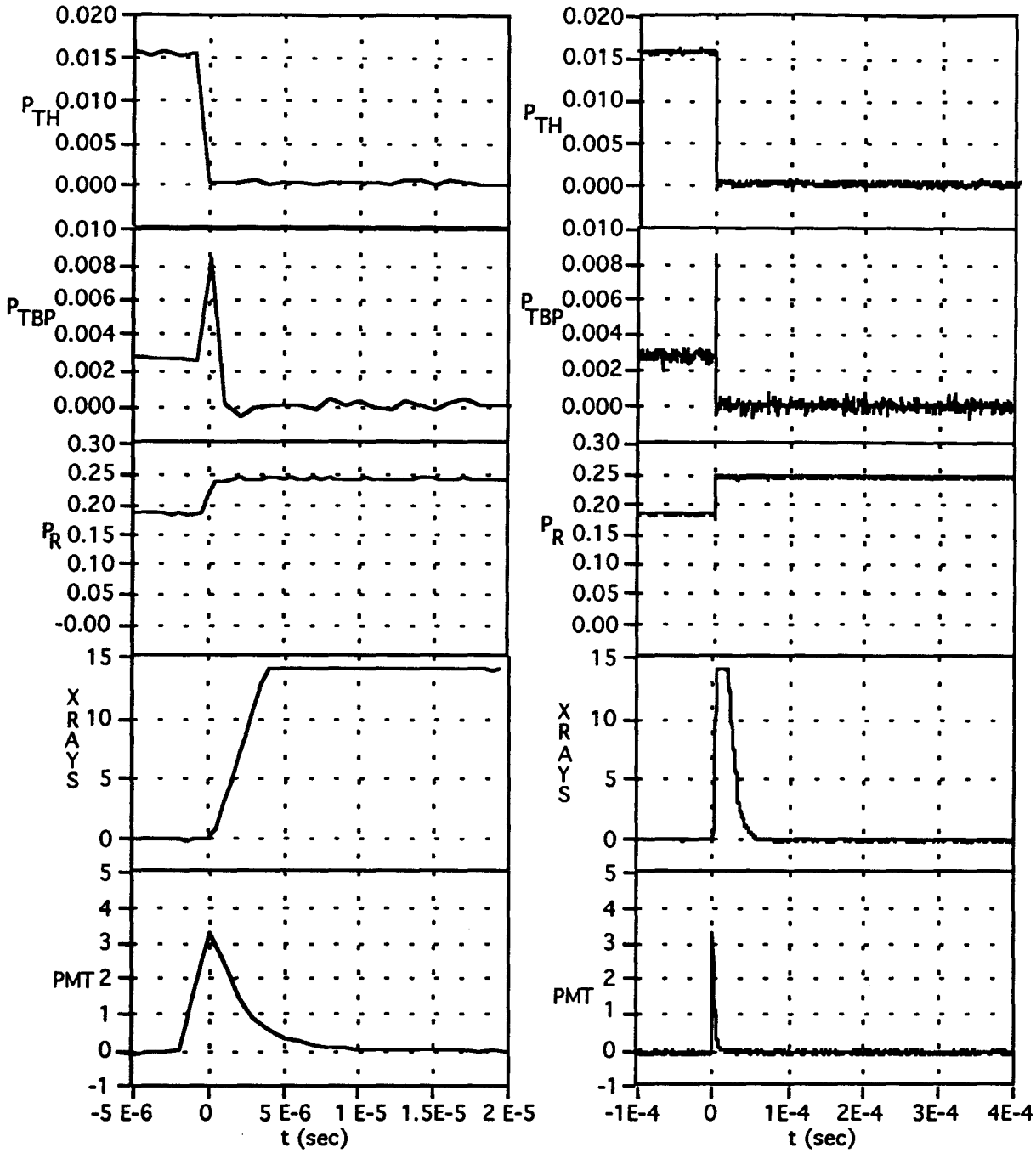

Figure 7. Transmitted power signal at the top hat probe (P_{TH}), transmitted power signal at the beam pipe probe (P_{TBP}), reflected power signal, x-radiation signal and PMT signal for an electronic quench of a cavity tested vertically. The data was taken at 1 Ms/sec. The signals shown on the left are the same event expanded to better show the timing for an electronic quench.

Electronic Quench

Figures 7 and 8 are examples of an electronic quench in the vertical and cryomodule configurations respectively. A long decay time tail of the light pulse, which was typically

5 ms, was observed when the gain of the PMT was increased. The stored energy is lost in less than 200 ns, and the cavity starts to refill with a time constant consistent with the loaded Q of the cavity (500 ms and 800 μs respectively). The x-radiation pulse measured in the vertical test is clipped due to the limited drive capabilities of the signal conditioning amplifier. Other data has been taken that indicates that this signal is approximately 1000 times larger than the steady state radiation of 500 Rad/hr emerging from the cavity while operated in the FE-regime. Additionally, pulsed x-radiation data taken during the cryounit tests, which made use of the scintillator-photomultiplier tube combination that provided much faster rise and fall times than the cold photodiode detectors used in the vertical tests, indicates that the x-radiation pulse is less than 1.75 μs FWHM. This time is also limited to the decay time of scintillator material.

An electronic quench is interpreted as the effect of the release of a large number ($\sim 10^{13}$) of electrons inside the cavity which are accelerated by the cavity and strike the cavity walls and beam pipe endplate. Several sources of the electrons are possible, two of which are photo emission due to x-radiation, and rf ionization of gasses which are photo desorbed due to x-radiation. One curious factor in these data is that, coincident with the PMT signal, the reflected power signal in the cryomodule test is rapidly reduced at the onset of the quench while the transmitted power rises quickly. This suggests that some process in the input waveguide or fundamental power coupler effectively increases the external Q of the input line. The increase in stored energy is quite short lived, however. Were the rise in P_T not present, one might interpret the decrease in reflected power as a type of beam loading.

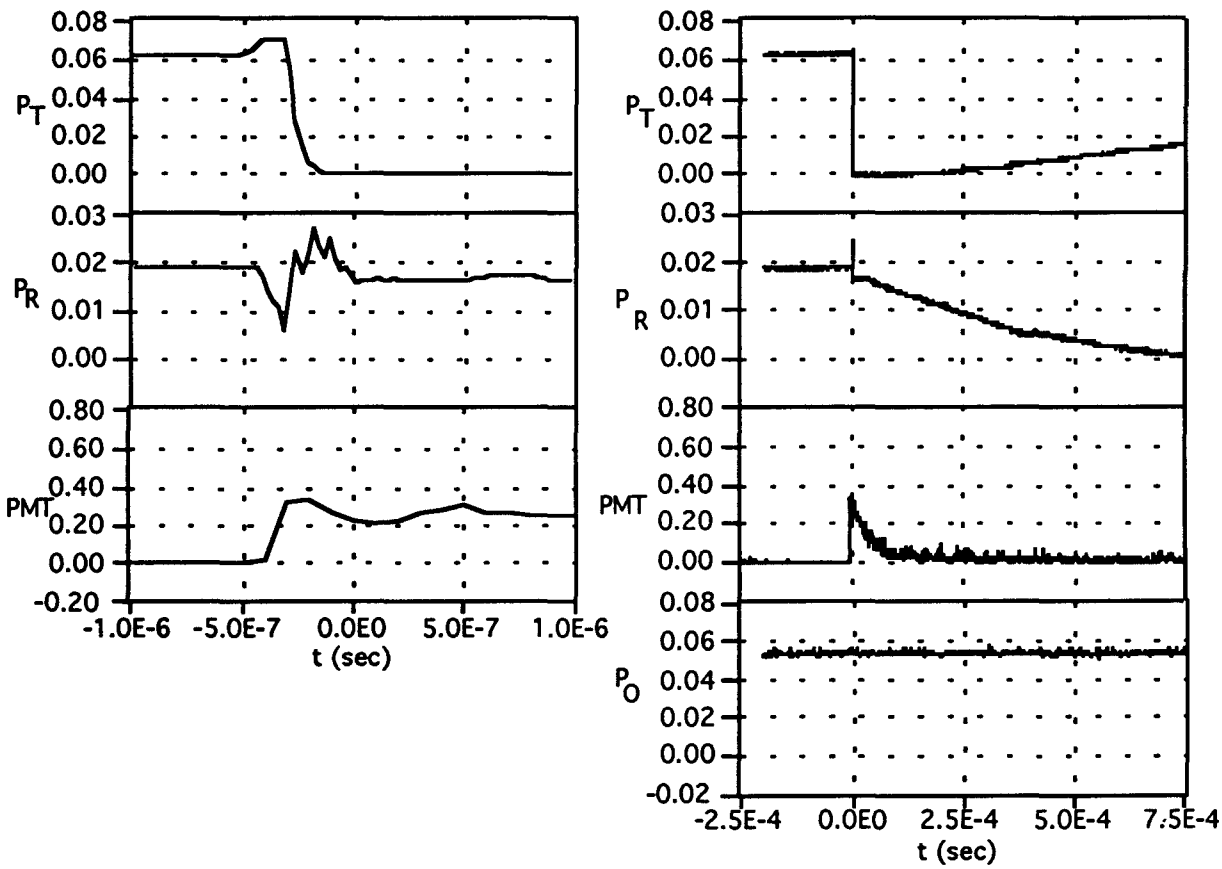

Figure 8 Typical signals for transmitted power (P_T), reflected power (P_R), PMT signal, and klystron drive signal (P_O) from an electronic quench in the cryomodule test. The signals shown on the left for the transmitted and reflected power signals are the same event expanded to better show the timing for an electronic quench.

Waveguide Vacuum Arc

Figures 9(a) and 9(b) are examples of another variety of event. In this type, a light pulse, with a broad band optical spectrum,[2] is sustained at a high level for a longer time, 450 μs in vertical tests, with a long tail lasting typically 5 ms. The x-radiation pulses in this type of event (as measured in the vertical tests) were typically an order of magnitude smaller than seen in an electronic quench. There are two striking differences between the two events (cryounit and vertical test) shown in Figure 9. The light pulse in cryounit event (a) is much more intense for the first 50 μs, while the klystron is on, and the light pulse in the vertical test event (b) is relatively constant after the initial 10 μs light pulse. Additionally, the decay of the transmitted power signal is much longer in the cryounit event than that observed in the vertical test event despite the much lower external Q on the cryounit test. Presumably some discharge in the waveguide system is preventing the stored energy in the cavity from propagating out of the waveguide. A similar (but possibly less dense) plasma in the vertical test event is apparently absorbing some of the cavity energy instead of reflecting it.

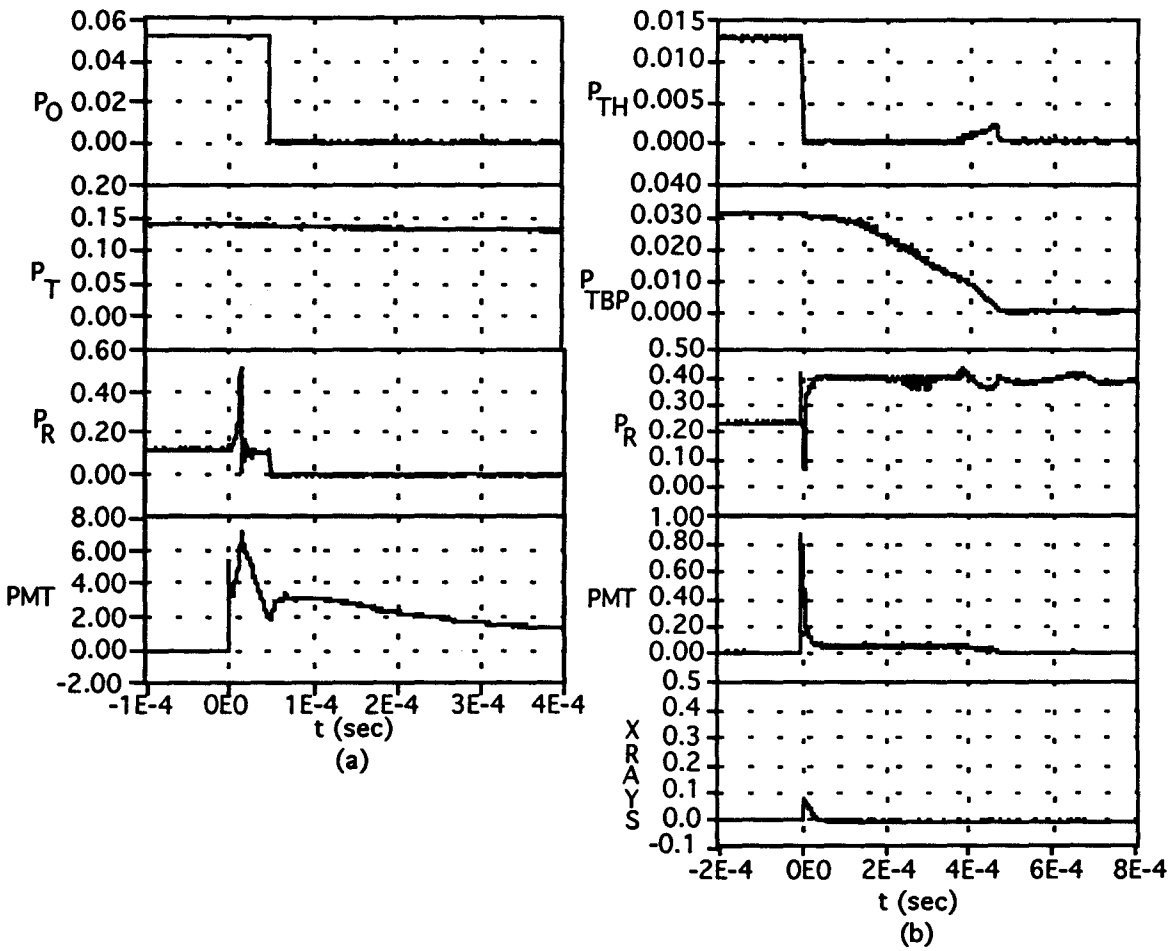

Figure 9. (a) Signals from a waveguide vacuum discharge in the cryounit test: klystron drive, transmitted power, reflected power, and PMT signals. (b) Signals from a waveguide vacuum discharge in a cavity tested vertically: transmitted power at the top hat probe (P_{TH}), transmitted power at the beam pipe probe (P_{TBP}), reflected power, PMT and x-radiation signals.

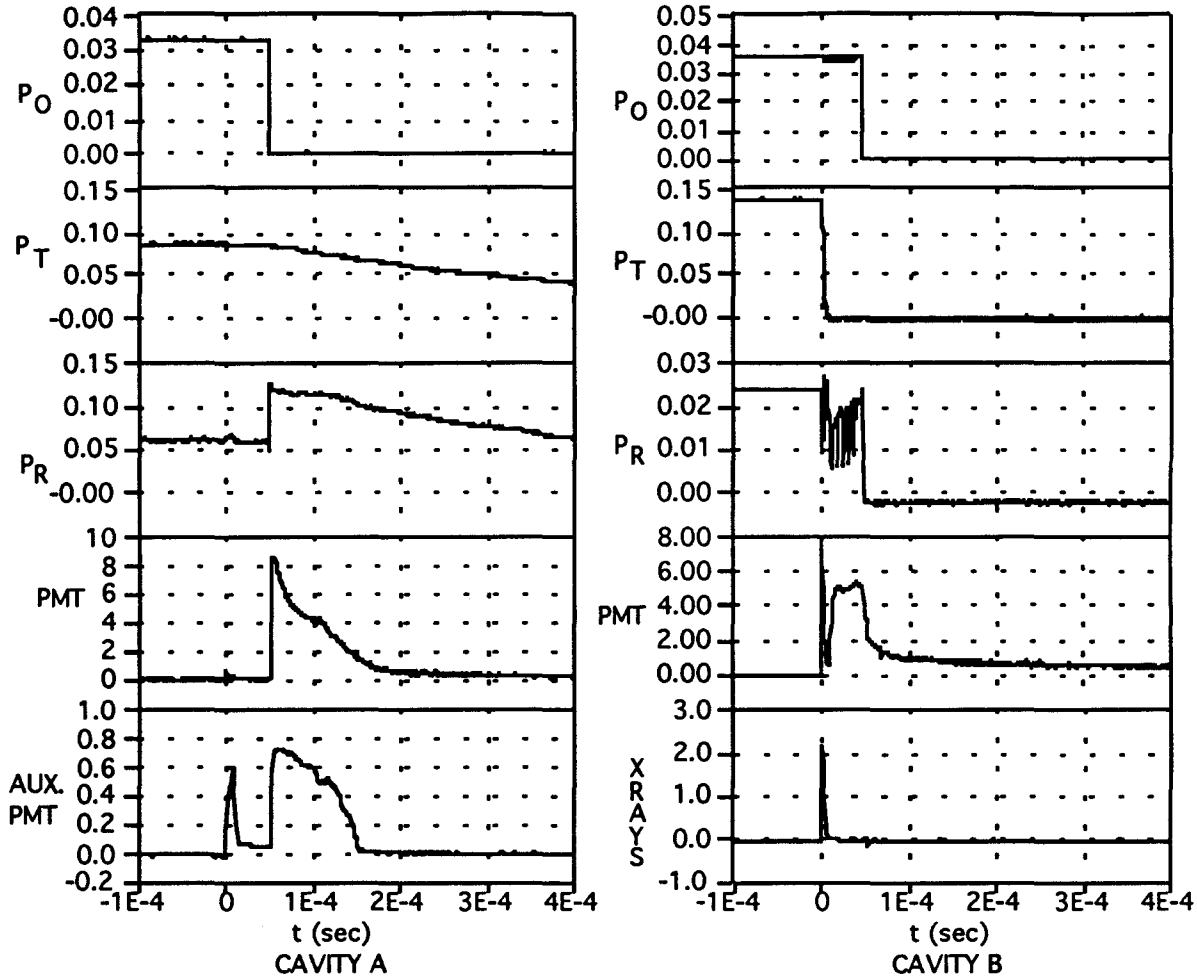

Figure 10. Signals from adjacent cavities during the same event. Klystron drive, transmitted power, reflected power and PMT signals for cavity A and B in the cryounit test showing (cavity B) an electronic quench with a waveguide discharge which is sustained by the klystron and (cavity A) a waveguide vacuum discharge which is initiated and sustained by the stored energy in the cavity. Additional signals are an x-radiation signal from a blanked off PMT placed near the end of the beampipe and the signal from a PMT viewing the cold window via the added view port which is shown in Figure 1.

Anomalous Events

Figure 10, cavity B, depicts a type of event that was seen often in the cryounit test. This type of event was initiated by an electronic quench which dissipates all the energy stored in the cavity in 8 μs. However, unlike the vertical tests, there was a discharge in the waveguide vacuum space which was sustained by the klystron (forward power of 2.2 kW) for an additional 40 μs. The x-radiation pulse depicted in this Figure is the signal from a blanked off PMT which was placed near the end of the beampipe at the cavity A end of the cryounit. This pulse was interpreted as optical emission from scintillation of the borosilicate glass which was used for the tube envelope.[8]

Figure 10, cavity A, depicts a waveguide vacuum discharge which was sustained by the energy stored in cavity A. In this event the klystron drive signal was turned off at t = 50 μs and a waveguide vacuum discharge started 5 μs later. The interesting data comes from the PMT which is looking directly at the cold window. This tube was biased at a lower voltage, 700 V versus 1000 V for the standard detectors. The pulse which was seen on this tube at t = 0 is attributed to x-radiation which was emitted from the cavity via

the cold window. An analysis of the x-radiation transmission characteristics, see Figure 11, shows that the energy spectrum of the radiation which would make it through the ceramic and sapphire windows but not through the Nb cavity wall, Cu heat shield and the stainless steel helium and vacuum vessels is between 10 keV and 100 keV. This suggests that some electrons in this energy range struck the cavity walls in the region of the fundamental power coupler. A likely source of these electrons was the electronic quench that occurred in cavity 8.

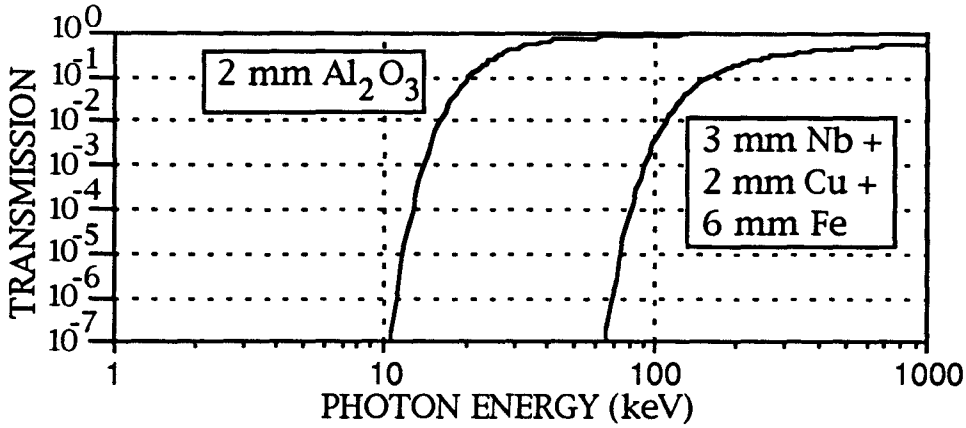

Figure 11, Theoretical transmission coefficient as a function of photon energy for 2 mm of Al_2O_3 and a combination of 3 mm of Nb, 2 mm of Cu and 6 mm of Fe. Data for calculation obtained from [9].

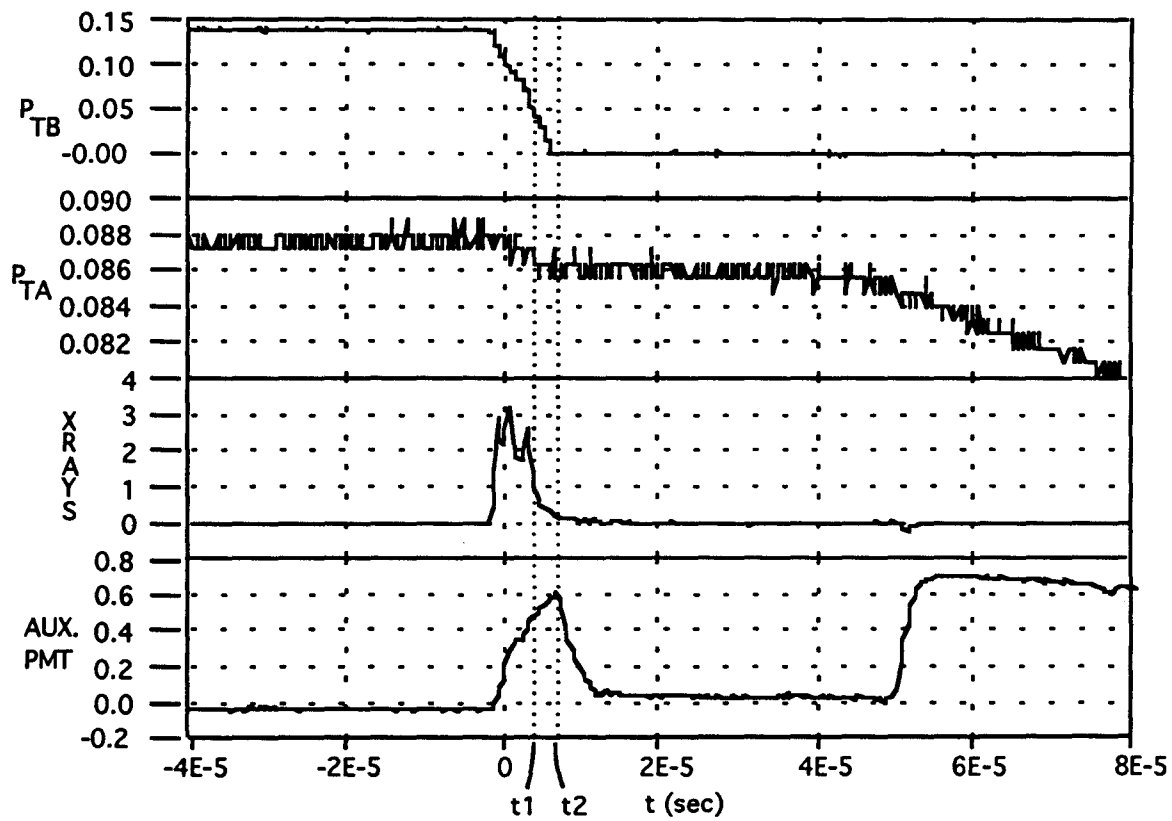

Figure 12 Expanded view of the transmitted power signals for cavities A and B, x-radiation signal and auxiliary PMT signal for the event shown in Figure 10.

Figure 12 shows an expanded view of some of the signals from Figure 10. One of the interesting features of this event is the sudden loss of 2% of the cavity stored energy, ≈ 0.25 J lost, coincident with the x-radiation pulse which is measured at the beam pipe at the end of cavity A. One explanation for this loss is that a portion ($n \approx 10^{11}$) of the electrons generated during the electronic quench ($n \approx 10^{13}$) in cavity B are captured by cavity A and accelerated by the field. The continued rise of the auxiliary PMT signal until t2 may be attributed to lower energy electrons which were not captured by cavity A. It should be noted that the cavities were operated at different frequencies ($\Delta f \approx 15$ kHz). Additionally, there is a correlation between the steady state x-radiation emission and the field level of cavity A when cavity B was operated in a field emission regime. As the field level in cavity A was increased with cavity B operated at a fixed field level the radiation levels observed at the beam pipe increased proportional to the square of the accelerating gradient in cavity A. This was interpreted as the capture and acceleration of field emitted electrons from cavity B by cavity A. This phenomenon is still under investigation.

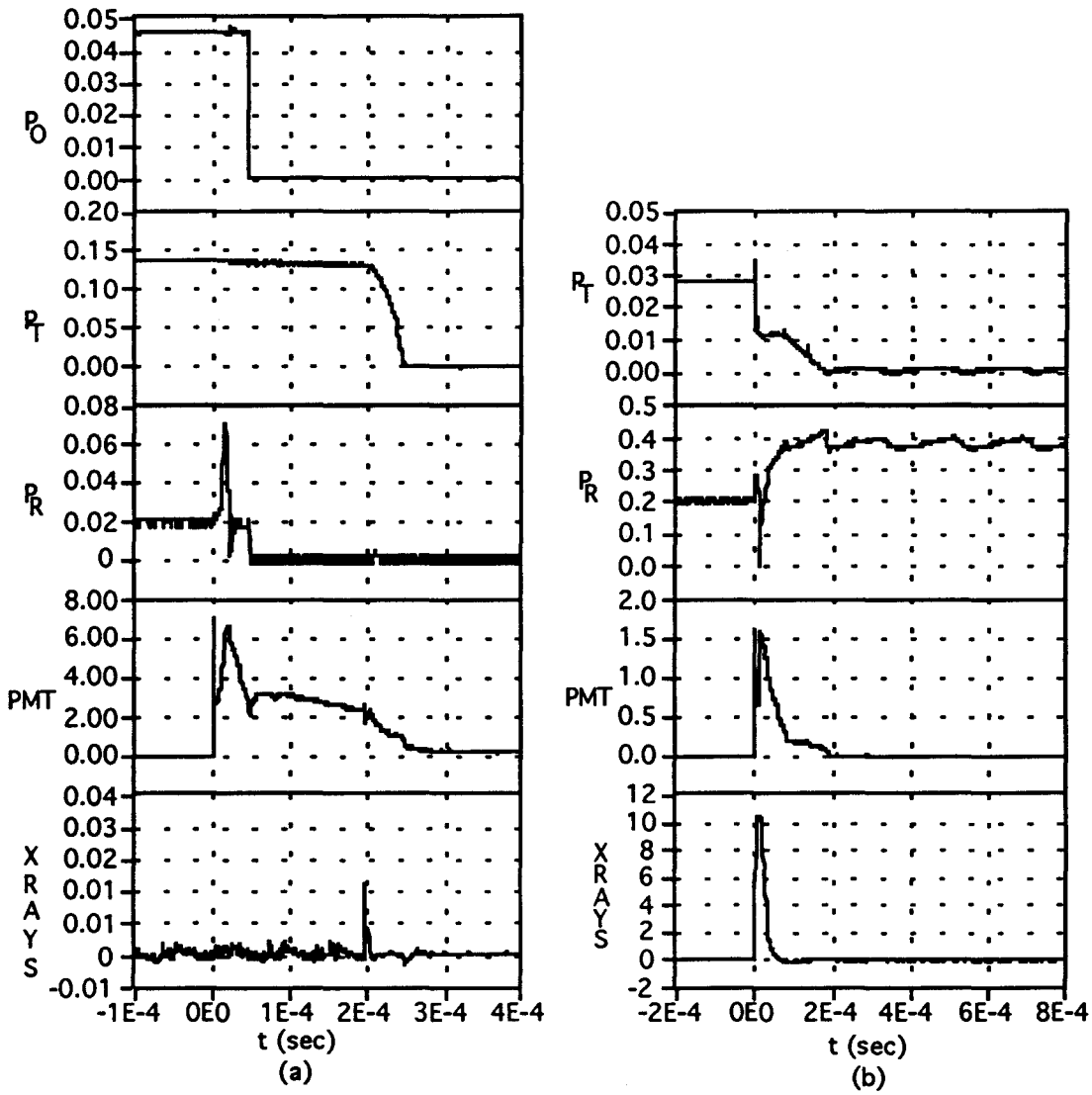

Figure 13. (a) Klystron drive, transmitted power, reflected power, PMT and x-radiation signal from a delayed electronic quench in the cryounit test. (b) Transmitted power, reflected power, PMT and x-radiation signals for a partial electronic quench followed by a waveguide vacuum arc in a vertical test.

Figures 13 depict variations of an electronic quench. In Figure 13(a) a waveguide vacuum discharge that, after 200 μs, transitions into an electronic quench in which the cavity stored energy is dissipated in 70 μs. This type of event was frequently seen in one of the 5-cell vertical tests and occasionally in the cryounit test. In Figure 13(b) an electronic quench dissipated only a limited amount of the cavity stored energy and the remainder is dissipated via a waveguide vacuum discharge.

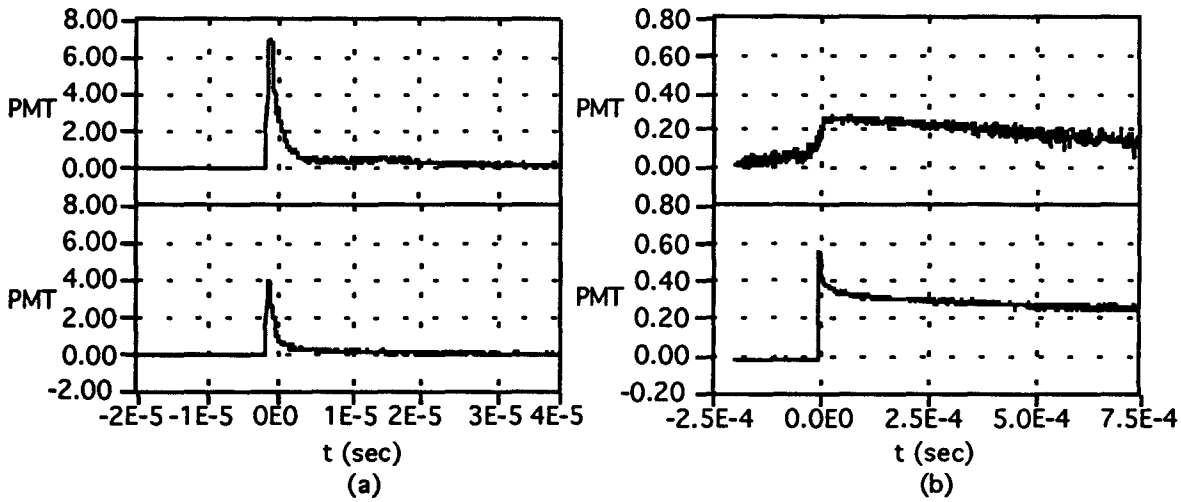

Figure 14. Typical light pulses without a quench which occurred in (a) the cryomodule test and (b) vertical testing. The top and bottom traces are different events.

Figure 14 shows light pulses without breakdown found in both the vertical and cryomodule tests. In both instances the transmitted power and reflected power signals show no measurable change which indicates that these events are not strongly coupled to the rf. The short pulses seen in Figure 14(a) are seen 3 to 10 times more frequently than waveguide vacuum discharges or electronic quenches. An expanded view of a waveguide vacuum arc, see Figure 15, shows that a similar pulse seems to be an initiator for the discharge. Spectroscopic studies indicate that this initial pulse in a waveguide vacuum arc has the same spectral characteristics as the light pulse emitted during an electronic quench.[2] The origin of these small light pulses is not understood and no spectral characterization has been performed. The longer pulses shown in Figure 14(b) do not affect the transmitted and reflected power signals. Data from the vertical tests indicates that the decay time of the light pulse is about 5 ms for this type of event. However, the power delivered to the cavities in the cryomodule by the klystron may be sufficient to sustain this type of discharge indefinitely.

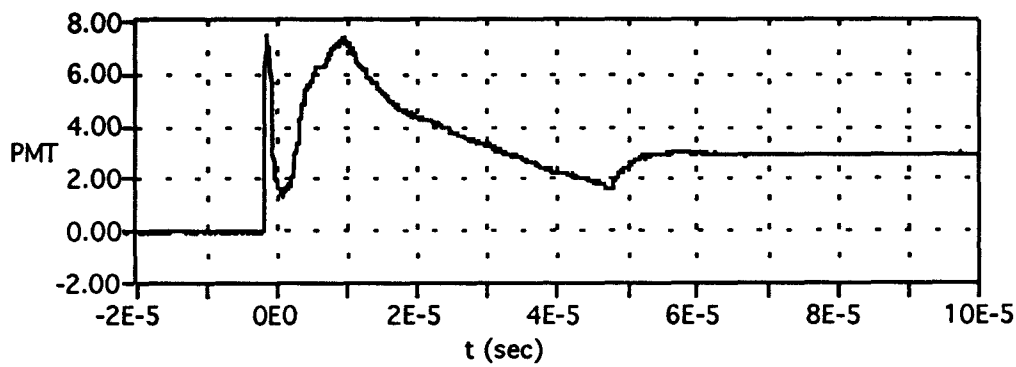

Figure 15. Expanded view of the PMT signal for a waveguide vacuum arc in the cryounit test. Note the similarity between the pulse at the beginning of the waveform and the pulses shown in Figure 14(a).

During the cryounit test the arcing rate (waveguide vacuum arcs plus electronic quenches) was monitored for the two cavities. No un-induced arcs were observed unless one of the cavities was operating with field emission. Cavity A, which did not show signs of field emission, produced a non-induced arc only once during the 70 hours of operation. Several waveguide vacuum discharges were produced, which did not occur until tens of microseconds after the rf drive was turned off after there was an arc in cavity B. Additionally, several arcs were observed which were attributed to control system transients. Both of these types of discharges were considered induced discharges. Discharges occurred in cavity B, at a rate proportional to the level of power dissipated due to field emission. This is shown in Figure 16. The arc rates were one arc every 14 hours when operated at 7.5 MV/m (1 W field emission loading), one arc every 18 minutes when operated at 9.7 MV/m (6 W field emission loading) and one arc every 11 minutes when operated at 10.5 MV/m (10 W of field emission loading). This trend is consistent with the model of arcs induced by a mechanism driven by free electrons or x-radiation.

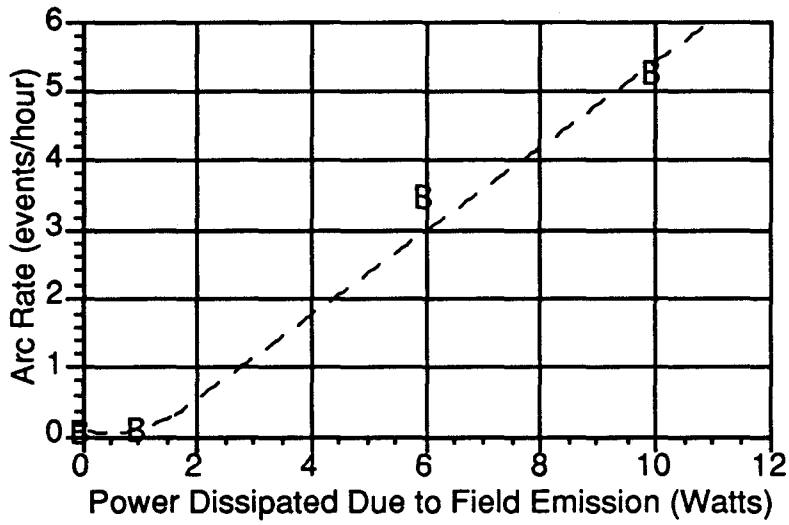

Figure 16. Arc rate versus field emission power for cavity B in the cryounit tests.

After all tests the windows were checked for through leaks. In the cryomodule and cryounit configuration the windows share a common vacuum manifold. It was not possible to distinguish between a leak in either window without disassembling the manifold which has the potential for degrading the cavity performance via the through leak. In the cryounit test the manifold leaked through to the cavity vacuum. In the cryomodule test one manifold out of four leaked through to the cavity vacuum. In the single-cell test and the oil drop test the window had a leak. In the 5-cell test the window had no leak. With the exception of oil drop experiment, the leaks were less than 10^{-6} Torr-l/sec, and the beamline vacuum integrity was maintained in the cryomodule configuration by combination of the polymeric window and the local 20 l/s ion pump. The exact mechanism for the origin of these leaks is not yet understood. However, all the windows which leaked were subjected to a heavy field emission environment.

Sensitivity to Control System Transients

The rf amplitude control circuit on one of the VCO subsystems in the cryomodule control room had a tendency to oscillate or was susceptible to noise. Additionally the VCO phase loop was marginally stable during the cryounit test. When the cavity was running at high field, these high power excursions often triggered an event, see Figure 17a. The problem seems to be related to the control signal for a PIN attenuator. Even at field levels below the onset of measurable field emission, arcs were induced by oscillations in the VCO

phase loop, see Figure 17b. These oscillations may be attributed to noise coupled into the marginally stable phase loop. The noise for both of these events was easily generated when a motorized phase shifter was operated. This type of problem could inhibit systematic conditioning studies. It is possible that some of the of arc trips in the CEBAF front end test may have been induced by rf control system bugs, which have since been corrected.

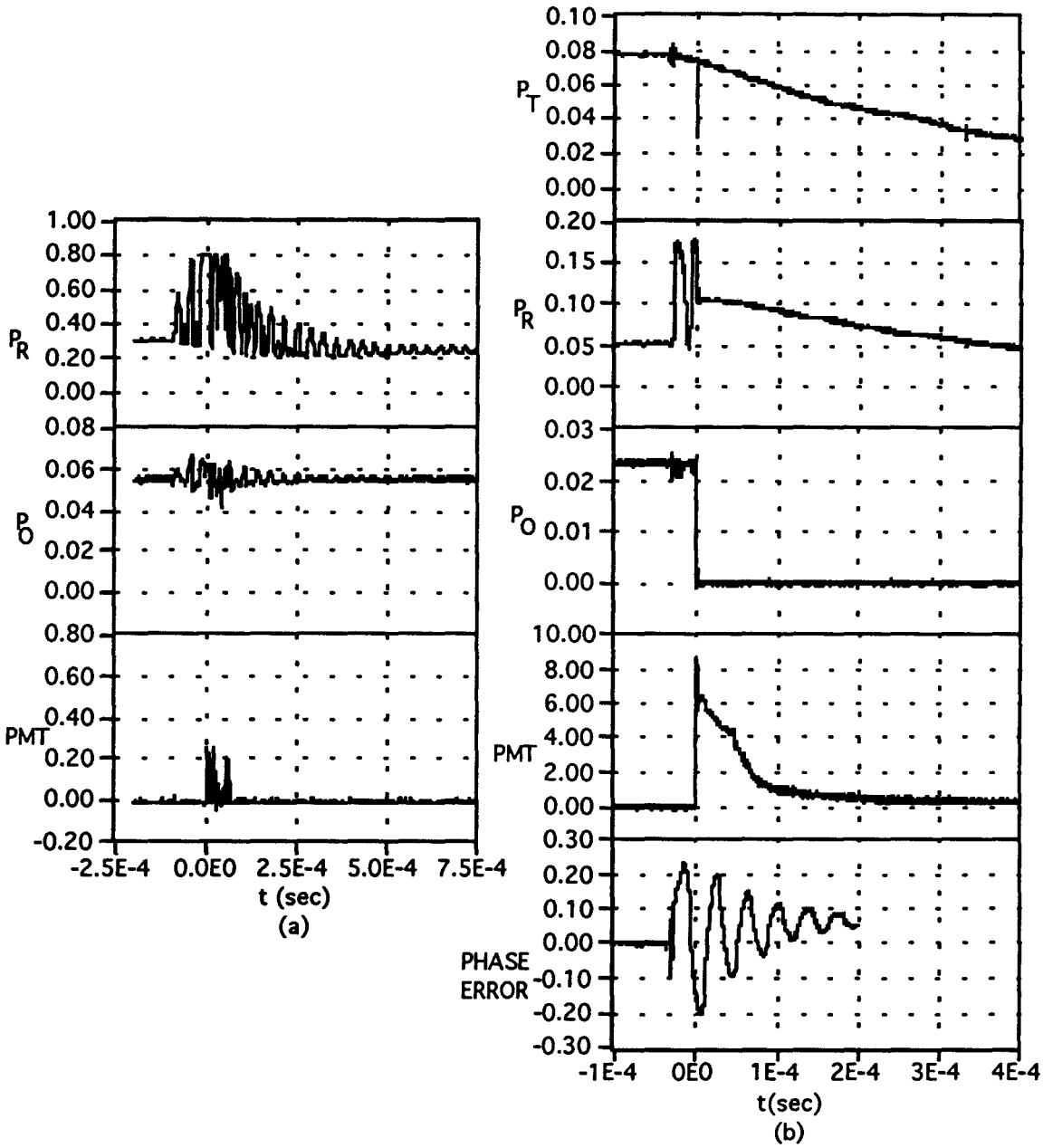

Figure 17. Typical signals for reflected power (P_R), klystron drive signal (P_O), transmitted power signal (P_T) and PMT signal for an event driven by rf control system instabilities. The data on the left demonstrates an amplitude loop problem while the data on the right demonstrates a phase loop oscillation. Note that there is no light emission for first excursions in the klystron drive, and phase error signals.

Impact on accelerator operations

At CEBAF an arc detector interlock fault invokes the fast shutdown system event causing beam loss for at least a few seconds. Additionally, an electronic quench which depletes a cavity of all stored energy would lead to beam loss at the spreaders on a sub-microsecond time scale before any interlock system has a chance to respond. While these studies have not produced a reliable predictor of the waveguide arcing or electronic quench rates, these events occur more frequently when the cavity is operated with heavy field emission or if there are rf control system instabilities. Arcing rates of 5 to 10 arcs per hour were not uncommon when the cavities were operated with heavy field emission where x-radiation levels exceeded 500 Rad/hr at the window frame. Preliminary data indicates that increasing the arc detector discrimination time from 2.5 μs to 50 μs should reduce the rate at which arcing interrupts accelerator operations by a factor of 3 to 10.

It is conceivable that the electron swarm, which we suspect is present in the cavity during an electronic quench, may propagate down multiple cavities. This would be recognized by the indication of a quench of several successive cavities or the beam loss monitor system responding in several locations at once. Such a propagation of a rapid quench from cavity to cavity could explain a phenomenon that has been observed at KEK.[10]

Conclusions

A few families of event types have been identified, and a consistent picture is emerging. The data taken during the tests using the cryomodule configuration are consistent in basic phenomenology with that taken in the vertical tests. All of the windows in cryomodule and cryounit tests were current production windows.

Several comments can be offered at this time concerning accelerator operations:

(1) The type of event that we have labeled "electronic quench" appears to be a relatively common phenomenon for cavities operated cw with heavy field emission loading, however, it was totally unexpected. Electronic quenches will not present a cryogenic load challenge, but they will cause transient beam loss in the spreaders.
(2) If the arc detector discrimination window is increased from 2 μs to 50 μs, the arc detector circuits will not detect the optical signal present during an electronic quench.
(3) It is quite conceivable that electronic quench could propagate over several cavities.
(4) If electronic quenches can be clearly discriminated, the reset to the quench interlock could be made rapid and automatic.
(5) Small leaks, (≈ 10-6 Torr-l/sec) which are evidently produced by arcing activity on the ceramic window, do not lead to a loss of beam time. However, they do require one to depend on the polymeric windows and guard vacuum ion pumps for primary beam line vacuum integrity.
(6) No amount of interlocks will prevent the energy stored in the cavity from flowing through the window after an rf shutdown. Since this is a substantial amount of energy (5 J @ 5 MV/m, 20 J @ 10 MV/m) the possibility of rf damage to the window cannot be eliminated by interlocks alone. (If in fact rf fields are relevant to window damage.)

Continuing these studies could be very useful in gaining additional understanding of the arcing problem as it may affect accelerator operations. The vertical tests with current production window materials and coatings will continue in order to determine if there is any arcing dependence on fabrication details. In addition to the work described here, other investigations are currently in progress including photoemission spectroscopy, field emission and secondary emission current measurements, DC-pulsed surface flashover, and DC bulk breakdown studies. The goal of these studies is to develop an adequate

understanding of the processes which contribute to arcing in order to then reduce, avoid, or eliminate these phenomena during accelerator operations.

References.

[1] Tom Powers, *et al.*, "RF Window Arcing Studies Update a Comparison of Results from Cryomodule 17 and Vertical Cavity Testing," CEBAF Technote TN93-030.
[2] Tom Powers, *et al.*, "Photoemission Phenomena on CEBAF rf Windows at Cryogenic Temperatures," Proceedings of this workshop.
[3] L. Phillips, *et al.*, "Some Operational Characteristics of CEBAF rf Windows at 2 K," Proceedings of the 1993 PAC conference May 1993.
[4] V. Nguyen-Tuong, J. Vac. Sci. Technol. A **11**(4), Jul./Aug. 1993.
[5] B. Fischer, "Untersuchungen an Supraleitenden 9-zelligen Prototyp Resonatoren für TESLA," Report University of Wuppertal, Fachbereich Physik, July 1992, Wuppertal, Germany.
[6] G. Ausust, "Multipactor Breakdown -- Lessons Unlearned", Proceedings of the AIAA 10th communications Satellite Systems Conference, Orlando, FL, March 1984.
[7] A. Woode, *et al.*, Microwave Journal, pp 142 - 155, January, 1992.
[8] H. Zagorities, *et al.*, "Gamma and X-ray Effects in Multiplier Phototubes," Proceedings of the IEEE Conference on Nuclear Radiation Effects, University of Washington, July 1964,
[9] W. McMaster, "Compilation of X-ray Cross Sections," Lawrence Radiation Laboratory report UCRL-50174-SEC-2-R-1.
[10] S. Noguchi, "Review of Progress in the Field of Superconducting Cavities," Proceedings of the Second European Particle Accelerator Conference, Vol. 1, 303 - 307, June 1990.

Acknowledgements

The work described in this paper involved part time effort from about 35 individuals in the SRF department spread over 18 months. We would like to acknowledge the assistance of John Brawley, Tom Elliot, Pete Kushnick, Bret Lewis, Ning Luo, Mark Taylor and the cryogenic support team for their efforts in the vertical tests. Additionally, we would like to acknowledge the support of Mike Drury, Kurt Macha, Jim Marshall, Joe Preble, Bill Schneider and the cryomodule support team for their effort in the cryomodule and cryounit tests.